

Geotechnical characterization of collapsible soils cemented by salts- A case study

G. Sotelo & S. Orellana

Knight Piésold Consultores S.A., Lima, Lima, Peru

J. Macedo

Georgia Institute of Technology, Atlanta, Georgia, USA

H. Jaffal, G. Espinoza, Z. Xu, K. Stokoe, C. El Mohtar

University of Texas at Austin, Austin, Texas, USA

ABSTRACT: Collapsible soils are typically found in arid regions and often have an aeolian or alluvial origin. In their natural state, they have a low moisture content and high initial or peak shear strength and stiffness due to their cemented structure (e.g. by the presence of salts). However, when these soils are subjected to wetting or saturation, the salts can dissolve resulting in a reduction of cementation and the peak strength and stiffness. This paper presents a summary of the geotechnical characterization performed on a deposit of collapsible soil at a proposed mine site near the southern coast of Peru, with particular emphasis on the dynamic characteristics. The site is located in a very high seismic area, which makes the dynamic characterization of these materials of primary importance. The geotechnical field investigation included drilling of boreholes, excavation of test pits, collection of samples, and execution of in-situ field tests. Undisturbed samples were carefully collected and oedometer, direct shear, consolidated drained triaxial, cyclic simple shear and resonant column tests were performed on them, while disturbed samples were also collected and tested for index properties and soluble salts content. The testing on undisturbed specimens was carried out at their natural moisture content state and after being subjected to wetting and the results revealed interesting insights in terms of the geotechnical properties and mechanical response of these materials as they lose the effects of salt cementation.

Keywords: Collapsible soils, low moisture content, undisturbed samples, static and dynamic conditions, wetting, strength reduction.

1 INTRODUCTION

This paper presents a characterization of certain collapsible soils based on field tests results and lab tests (under static and dynamic conditions). Collapsible soils are metastable in that they contain relatively large voids within a skeleton of grains that are cemented together by salt precipitate residues. Their grain sizes range from silt to sand. In a dry state, these soils have a relatively high peak strength and initial stiffness but in the presence of water the precipitate bonds between grains can dissolve causing the loose, high void ratio structure to collapse, producing deformations which may cause the failure of a structure. Collapse can also be triggered by static shear stresses or earthquake loading. This case of study consists of collapsible soils that are located on the southern coast of Peru in an arid and highly seismic region. In this particular case, a Tailings Storage Facility (TSF) will be founded on the site of these soils and their characterization has been used to determine the foundation design approach for the TSF.

The local ground conditions consist of alluvial and aeolian deposits up to 13.0m thick that include collapsible soils that were formed by the accumulation of sediments in a dry and evaporative environment.

Based on a probabilistic seismic hazard study, the area is characterized as highly seismic and forms part of the Pacific Ring of Fire. The regional tectonic framework on a larger scale is governed by the interaction of the Nazca and South American plates. The border between the Nazca plate and the South American Plate in this region is demarcated by the Peru-Chile trench, which is 90 km west of the Peruvian coast near the region where the site study is located. The continuous subduction of the Nazca plate along the Peru-Chile trench is the main source of large earthquakes ($M > 7.0$).

Significant collapse-induced deformations are a concern due to the considerable thickness of the collapsible soils and the seismicity of the site, and therefore the design requires an understanding of the collapse mechanisms and pre and post collapse geotechnical properties of the soils.

2 GEOTECHNICAL SITE INVESTIGATION PROGRAM

A geotechnical site investigation was performed in the area of study where the collapsible soils are located. The site investigation consisted of 39 boreholes and 152 tests pits executed between 2007 and 2017 including in-situ field testing and sampling. Figure 1(a) shows the geotechnical site investigation map. During the investigation, undisturbed and disturbed samples were extracted to develop a geotechnical laboratory test program for the material characterization. The undisturbed samples were obtained from block samples in the tests with block sizes of approximately 300 millimeters [mm] x 300 mm x 150 mm. These samples were used to perform advanced tests such as: oedometer consolidation, direct shear, consolidated undrained and consolidated drained (CU/CD) triaxial, resonant column and cyclic direct simple shear (CDSS) tests. Additionally, disturbed samples were collected from boreholes and tests pits for index testing that consisted of Atterberg limits, particle size distribution with hydrometer tests, specific gravity and soluble salts content.

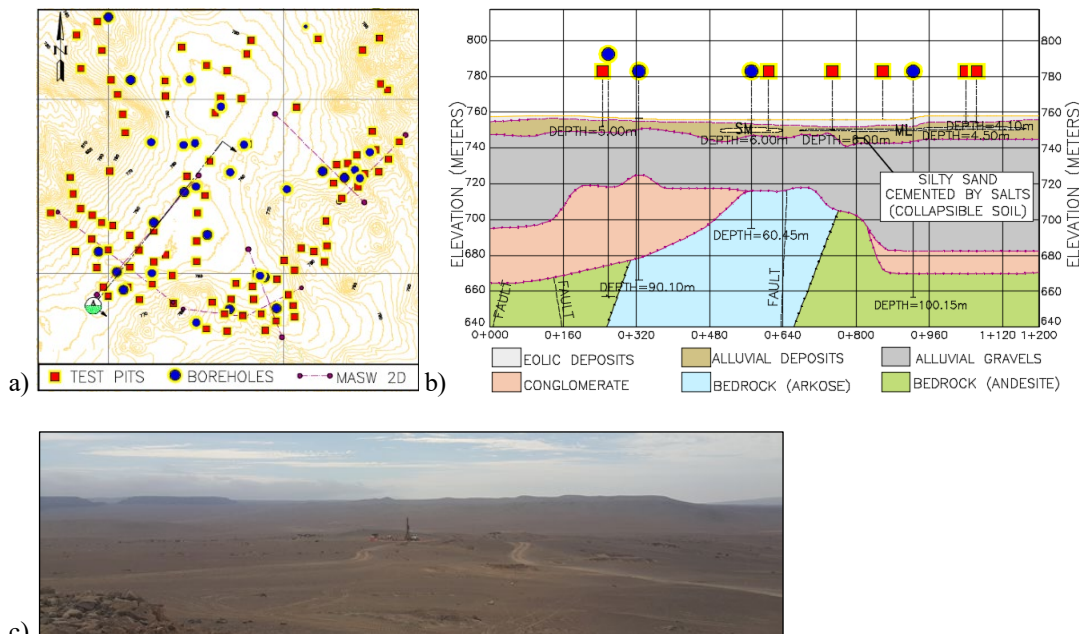


Figure 1. Site Investigation a) Map b) Section c) Panoramic view

In-situ field testing included Standard Penetration Tests (SPT), shear wave velocity measurements using Multichannel Analyses of Surface Waves (MASW) and downhole permeability tests (Lefranc tests). SPTs were performed in dry conditions (in-situ condition), giving a compactness of moderately dense to dense (blow count numbers ranged from 24 to refusal), and in wet conditions, where the compactness was loose to dense (blow count numbers between 3 and refusal). Figure 2(a) presents corrected blow count numbers (N_{160}) versus depth in wet conditions (after flooding of the borehole artificially, in advance of the subsequent SPT test) to represent conditions after potential collapse due to dissolution of salts. Under dry conditions, the majority of results were at refusal. Wet conditions were created floating the borehole during saturation in permeability tests (prior to SPT tests) and 2-3 additional hours of saturation. It is important to note that thorough/complete wetting was not achieved in all SPTs, and some results give high blow counts as a result that likely still represent a “pre-collapse” stiff condition. The dilative-contractive boundary for wetted “post-collapse” soils during shearing was assessed using correlations based on the (N_{160}) values obtained from the SPT testing and the effective

stress conditions following the procedures proposed by Fear and Robertson (1995) and is plotted on Figure 2(a). This shows that the wetted “post-collapse” soil is primarily dilatant (i.e. it would tend to increase its volume generating negative pore pressures under shearing), and in few cases, contractive behavior (i.e it may tend to decrease its volume generating positive pore pressures under shearing). This suggests that upon collapse, much of the soil crosses the Critical State Line from contractive to dilatant behavior. Cone penetration tests were not possible due to refusal at the surface.

MASW results showed that shear wave velocity measurements (V_s) varied between approximately 230 and 450 m/s with some values as high as 690 m/s in the zones with major salt cementation (Figure 2(b)). The hydraulic conductivity of the soils obtained from the permeability tests can be classified as low to medium, with values ranging from 10-3cm/s to 10-2cm/s as shown in Figure 2(c).

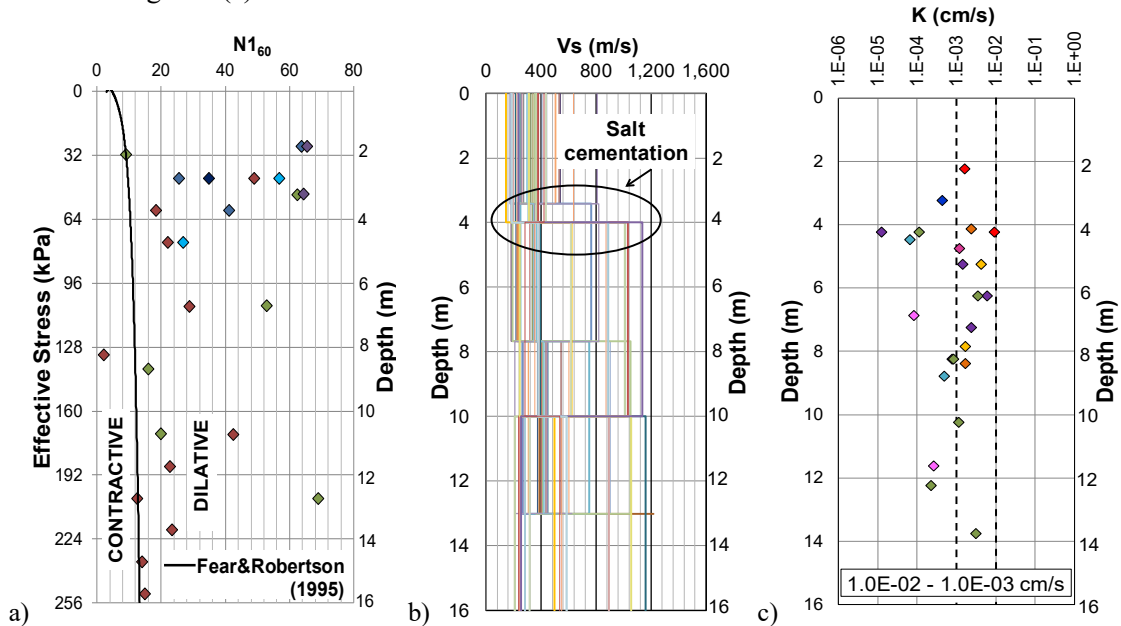


Figure 2. Field parameters vs effective stress/depth a) N160 Blow counts number, b) Shear wave velocity measurements and c) Hydraulic conductivity

3 COLLAPSIBLE SOILS CHARACTERIZATION

3.1 Index properties

Index properties such as gradation, moisture content, salts content and collapse index were obtained in order to gain more understanding of this challenging material. The soil in this study is typically classified as silty sand (SM) and poor graded sand (SP) based on ASTM 2487 USCS classification. It has no plasticity and very low natural moisture content. Figure 3 and Table 1 show the range of particle size distribution curves obtained and the remaining Index Properties tested for.

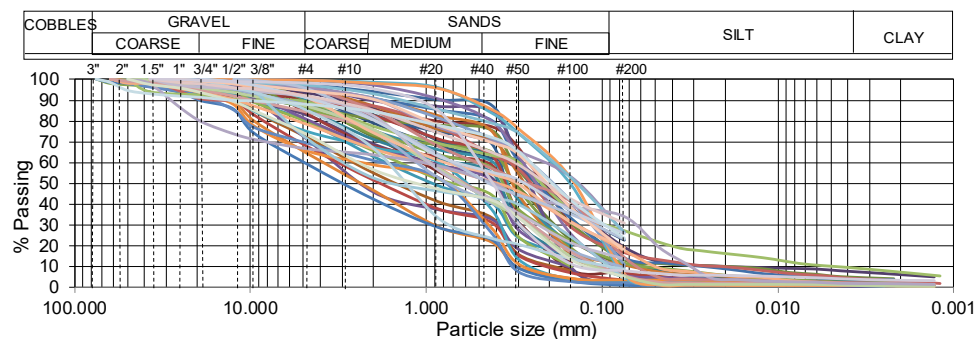


Figure 3. Collapsible soils gradation

Table 1. Collapsible soils properties

Origin	USCS	Gravel%	Sand%	Silt/Clay%	LL	PL	PI	w%	Gs
Alluvial deposits	SM,SP,SP-SM	5-15	30-85	6-30	NP	NP	NP	1-5	2.6-2.9

During the site investigation, the material identified as the collapsible soil was sub-divided in two types, A and B (A over B). Collapsible Soils Type A are looser with a void ratio varying from 0.8 to 1.2, with an estimated relative density between 50% and 60% and a thickness between 4.0 and 10.0m. Whereas, Collapsible Soils Type B are denser with a void ratio less than 0.7 and an estimated relative density higher than 80%. These soils are located deeper than 10.0m; however, they were also found at 6.5m depth in other zones according to stratigraphic and deposition of this material. Figure 4 shows the variation between the void ratio and depth for the two types of collapsible soils.

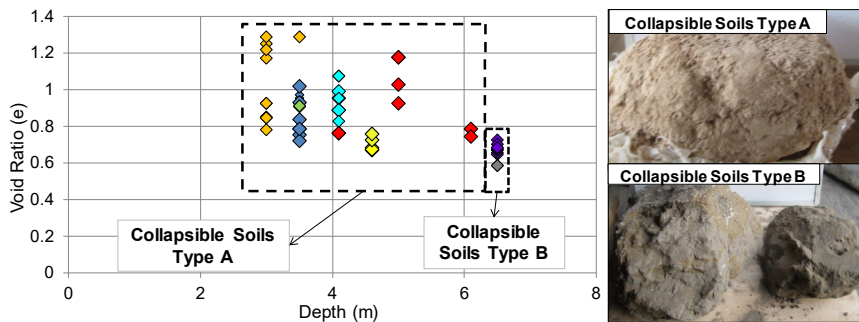


Figure 4. Void ratio vs depth for Collapsible soils type A and B.

4 COLLAPSABILITY AND SALT CONTENT

In order to assess the collapsibility of these soils, the standard test method for measurement of collapse potential of soils (ASTM D5333-03) was conducted to obtain the collapse index (Ie). Ie is defined as the strain after wetting (in percent minus) the strain before wetting (in percent), at a vertical stress of 200kPa, measured using a conventional 1-D oedometer cell. For Collapsible Soils Type A, the Ie varied from 0.7% and 14% making its degree of collapse slight to moderately severe; meanwhile for Collapsible Soils Type B, the Ie was found between 0.4 and 0.5%, classifying its degree of collapse as slight. The complete results from these tests are presented in Figure 5 (a).

Precipitate salts were identified as the cementing agent helping the soil particles to bind into a brittle structure. Standard test NTP 339.152 was conducted to quantify salts content. Figure 5(b) shows the variation of void ratio vs salt content. Figures were plotted using the void ratio since this parameter was used to characterize both types of collapsible soils.

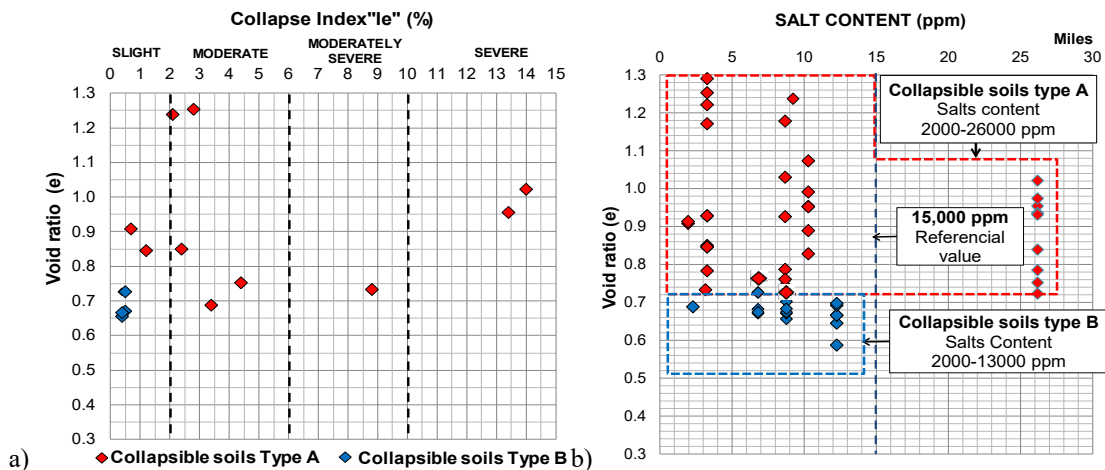


Figure 5. Collapsibility parameters vs void ratio a) Collapse Index, b) Salt Content.

5 SHEAR RESPONSE OF COLLAPSIBLE SOILS

The shear behavior of these collapsible soils was investigated using different lab tests: Direct Shear (ASTM D3080), Consolidated Undrained Triaxial (CU) (ASTM D4767-95) and Consolidated Drained Triaxial (CD) (ASTM D2850).

5.1 Direct Shear Test (ASTM D3080)

Direct shear tests were performed on undisturbed specimens at different normal confining stresses for Collapsible Soils Type A and B. The testing procedures were modified from the standard method to account for the unique nature of this material. Specifically, after applying the vertical stress, collapse was induced through wetting of the samples. The vertical deformations were monitored with time, and horizontal shearing was initiated only after cessation of vertical deformation (i.e., at the end of the settlement). Thus, the shear behavior and strength was on the “post-collapse” material. Figure 6(a) shows the failure envelopes from these tests. The measured effective stress friction angles were $\phi' = 31^\circ$ and 36° for Collapsible Soils Types A and B, respectively and no cohesion was observed, as expected.

The horizontal versus vertical displacements recorded during shearing are presented in Figure 6(b). Collapsible Soil Type A exhibited contractive behavior over the ranges of normal stresses tested while Collapsible Soils Type B, at normal stresses of 200kPa and 400kPa exhibited dilative behavior but them at 800kPa it exhibited contractive behavior. These results compare well with the relative densities of the materials presented above. Collapsible Soils Type A is loose with $D_r=50\%$ - 60% and is contractive; and Collapsible Soils Type B are dense with $D_r=80\%$ and are primarily dilative but become contractive at higher normal stresses, as expected.

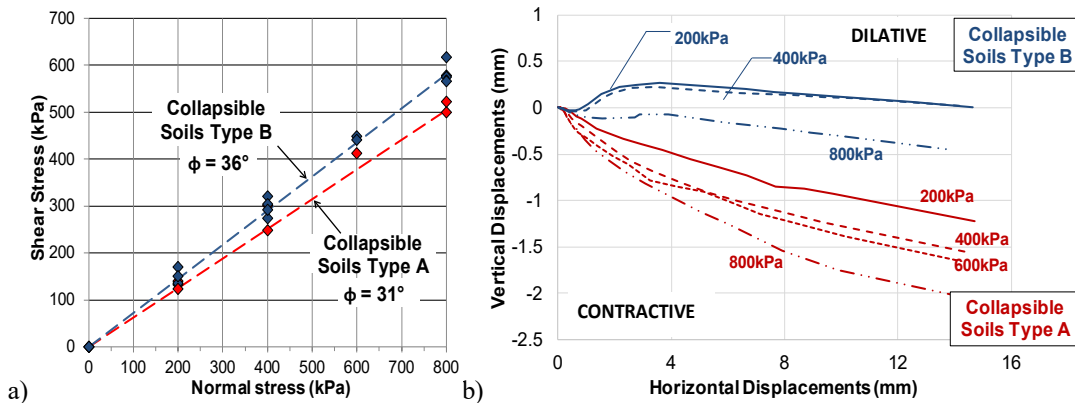


Figure 6. Direct Shear tests results for Collapsible soils A and B. a) Failure envelopes, b) Horizontal versus vertical displacements.

5.2 Consolidated Undrained (CU) and Consolidated Drained (CD) Triaxial Tests (ASTM D4767-95 and ASTM D2850)

CU and CD triaxial tests were performed on undisturbed specimens of Collapsible Soils Type B. Given the loose compactness of Collapsible Soils Type A, no undisturbed block was possible to be extracted for running these tests on them. These tests were performed to determine the behavior of the material (dilative or contractive), and the change in strength as the soil goes from a “pre-collapse” undisturbed (cemented) state to a “post-collapse” state (either by wetting or remolding).

The stress paths from the CU triaxial tests are plotted in Figure 7. As noted, the material has a dilative response during shearing for all the tested effective stresses. Since pore pressure response depends on relative density and confining effective stress, the material’s tendency to generate pore pressure will increase for higher confining stresses.

CD triaxial tests also were performed in different conditions in order to evaluate how the effect of collapse affects the strength and stiffness or compressibility parameters. The conditions were:

- a) On undisturbed specimens (U): Specimens at natural water content without any flushing.

- b) On undisturbed flushed specimens (F): The specimens were flushed prior to back pressure saturation with 3 and 9 pore volumes (3PV and 9PV). For the 9PV, 3 pore volumes were flushed at 3 stages spaced at 2 hours. The objective is to ensure the large majority of salts were flushed out before testing (Collapse condition).
- c) On Reconstituted Crushed (RC) and Reconstituted Washed specimens (RW): For the “crushed sand specimens”, the undisturbed specimens were crushed using a rubber mallet with the salt kept in the sand and finally reconstituted and for the “washed sand specimens” the materials were crushed and then washed to re-move the salt (without losing any of the fines) and finally dried. In both cases, the specimens were compacted at the original dry density of the undisturbed specimens.
- The specimens tested as CD were labeled: “Sample 1” (S1), “Sample 2” (S2) and “Sample 3” (S3), based on the location of block samples they were extracted from.

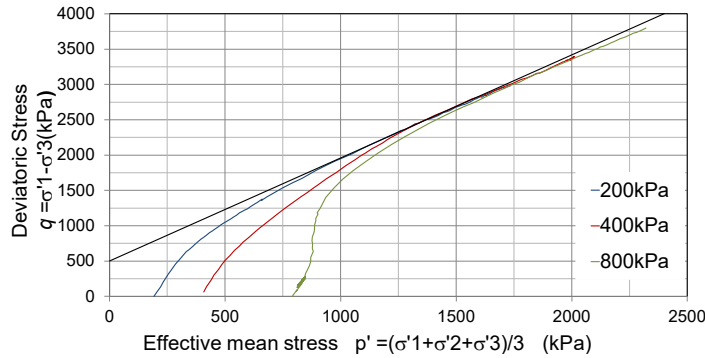


Figure 7. p' and q parameters from CU triaxial tests.

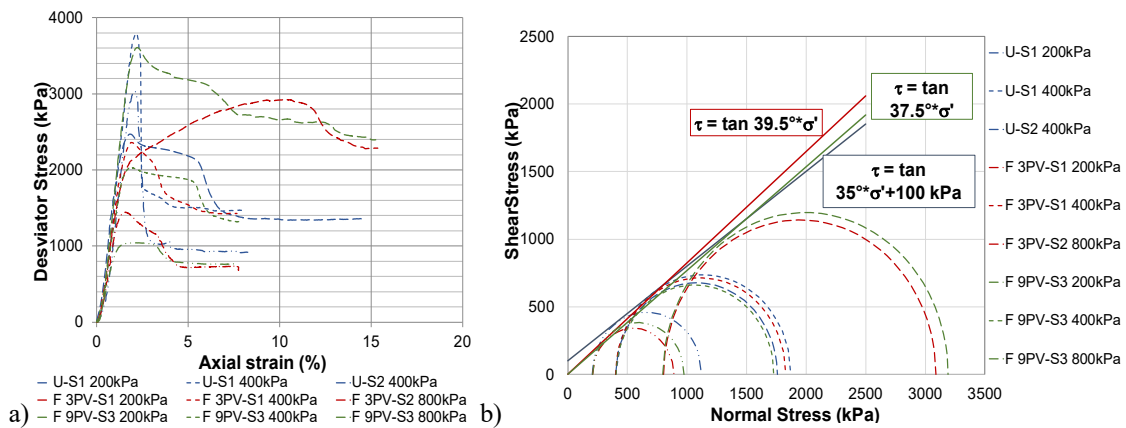


Figure 8. CD triaxial testing results of undisturbed dry, flushed with 3PV (Samples 1 and 3) and flushed with 9PV (Samples 1 and 3) specimens. a) Deviatoric stress vs axial strains; b) Residual failure envelopes

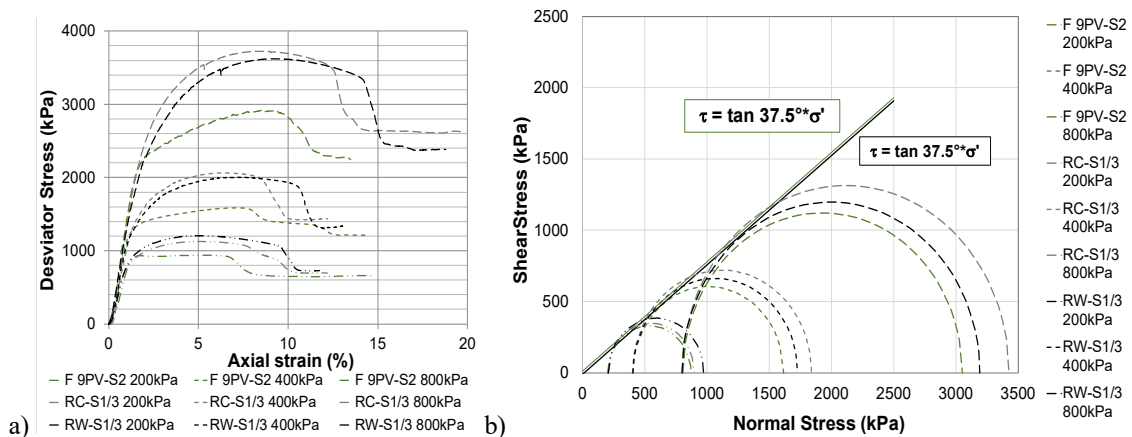


Figure 9. CD triaxial testing results of undisturbed flushed with 9PV (Sample 2), reconstituted RW and RC specimens. a) Deviatoric stress vs axial strains; b) Residual failure envelopes

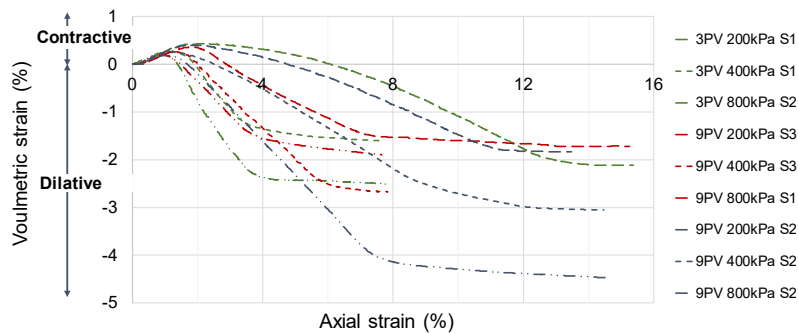


Figure 10. Volumetric strain vs axial strain for flushed 3PV specimens (Samples 1 and 3) and 9V specimens

The results from the CD triaxial testing were grouped and plotted in Figures 8, 9 and 10. The shear stress-strain and strength parameters are shown in Figures 8 and 9 and the strength parameters are for the large-strain (residual) strength condition. The flushing/reconstitution process can be seen as having a minimal impact on the residual strength since all the samples were in a “post-collapse” modified structure (at least on the failure plane) by either backpressure saturation (undisturbed specimens), flushing (3PV-9V flushed specimens), or crushing and washing (crushed and washed specimens). This means that despite the process applied, all specimens arrived at a similar “post-collapse” condition, which suggests that the residual deviatoric stresses are similar for the same confining stress. This is consistent with the Critical State approach (Jefferies & Been, 2015).

Contrary to common residual strength, the peak stresses were found to be strongly affected by the initial conditions. Figure 8(a) shows that the undisturbed dry specimens exhibited higher peak deviatoric stresses than the 3PV flushed specimens, and the 3PV specimens in turn, exhibited higher peak deviatoric stresses than the 9PV flushed specimens. This suggests that as more water flushing occurs, more salt is washed out, which reduces the remaining cementation and causes the specimens to fail at lower peak strengths. For the crushed and washed specimens, the loss of cementation was found to not only reduce the peak strength, which were comparable with 9PV flushed specimens, but also to reduce the initial stiffness or modulus. Crushed and washed specimens were found to present an initial stiffer response and then a gradual decrease in stiffness to the peak strength; meanwhile, for undisturbed or flushed specimens, the initial stiffer phase remained largely intact until the peak stress was reached.

Specimens extracted from Samples 1 and 3 exhibited different behaviors during shearing compared to those obtained from Sample 2. As observed in figures 8(a) and 9(a), specimens from Samples 1 and 3 experienced a major drop in strength after reaching peak strength at strains between 1% and 2%, indicating a quite brittle behavior. Specimen from Sample 2 on the other hand, experienced a lower peak strength at larger strains between 5% and 10% and experienced a more gradual drop to residual strength. As illustrated in Figure 10, specimens from Sample 2 were more contractive than those from Sample 1 and Sample 3, at the same confining stress. These results are consistent with the lower shear strength recorded for the Sample 2 specimens.

6 CYCLIC BEHAVIOR

As described in the introduction, the material is located in an area with very high seismicity, making it critical to study its dynamic properties and behavior under cyclic loading. The cyclic behavior was focused on Collapsible Soils Type B. Should a TSF be founded in the area of study, it is likely that the shallower Collapsible Soils Type A would require excavation prior to construction of the facilities.

6.1 Dynamic properties

These tests were performed on undisturbed specimens (U) at their natural moisture content and on reconstituted washed specimens (RW) from Sample 1 and Sample 2 (these were prepared

following the same procedures used to prepare the CD triaxial washed specimens). The specimens were placed in a resonant column device and tested for Maximum Shear Modulus (G_{max}) and Minimum Material Damping Ratio (D_{min}), as well as the variation in shear modulus and damping with shear strain during loading, unloading and reloading.

G_{max} was determined based on the equation shown Figure 11, where A_g and n_G are known as fitting parameters that depend on the characteristics of the material. The fitting parameter “ A_g ” is dependent on the sand fraction properties (gradation, angularity, composition, and average particle size) and specimen properties (void ratio, density, and cementation). The drop in this value from 535 to 96 MPa for the same sand composition and same density (for the reconstituted specimen) is a measure of the breakage of cementation. The parameter “ n_G ” is a measure of the increase in G_{max} with effective stress. For typical sands, this number is approximately 0.5 (range between 0.45-0.55), and this compared well with the value obtained for the reconstituted specimen (0.47). The undisturbed specimens had an “ n_G ” value of 0.28, which is very low relative to literature values for materials of similar index composition. This low value indicates that the change in shear modulus is not as influenced by changes in confining stress as it would typically be in a normal clean sand. The cementation is a major contributor to stiffness and is not nearly as affected with increase in confining pressure. Therefore, a lower n_G value, combined with a high A_g , is a direct result of the high salt cementation in the undisturbed specimens.

The G_{max} and D_{min} values decrease in the absence of cementation (i.e. after flushing and remolding), with the difference in D_{min} decreasing at higher confining stresses (Figure 11(a) and 11(b)). Figures 11(c) and 11(d) show the variation in shear modulus, and normalized shear modulus and damping ratio with shear strain, respectively, at 414 kPa effective confining stress. Figure 11(c) shows that a major drop occurred in shear modulus between the “U” specimen and the “RW” specimen. The normalized modulus results (Figure 11(d)) show a similar non-linear response between the “U” specimen and “RW” specimen from Sample 1, whereas the “U” specimen from Sample 2 shows slightly higher non-linearity. The upper and lower curves of G/G_{max} and Damping, as reported by Seed and Idriss (1970), are included in Figure 11(d) for comparison. The measured data are near the upper boundaries for the G/G_{max} and Damping relationships. These results are expected considering the high relative density of the sand.

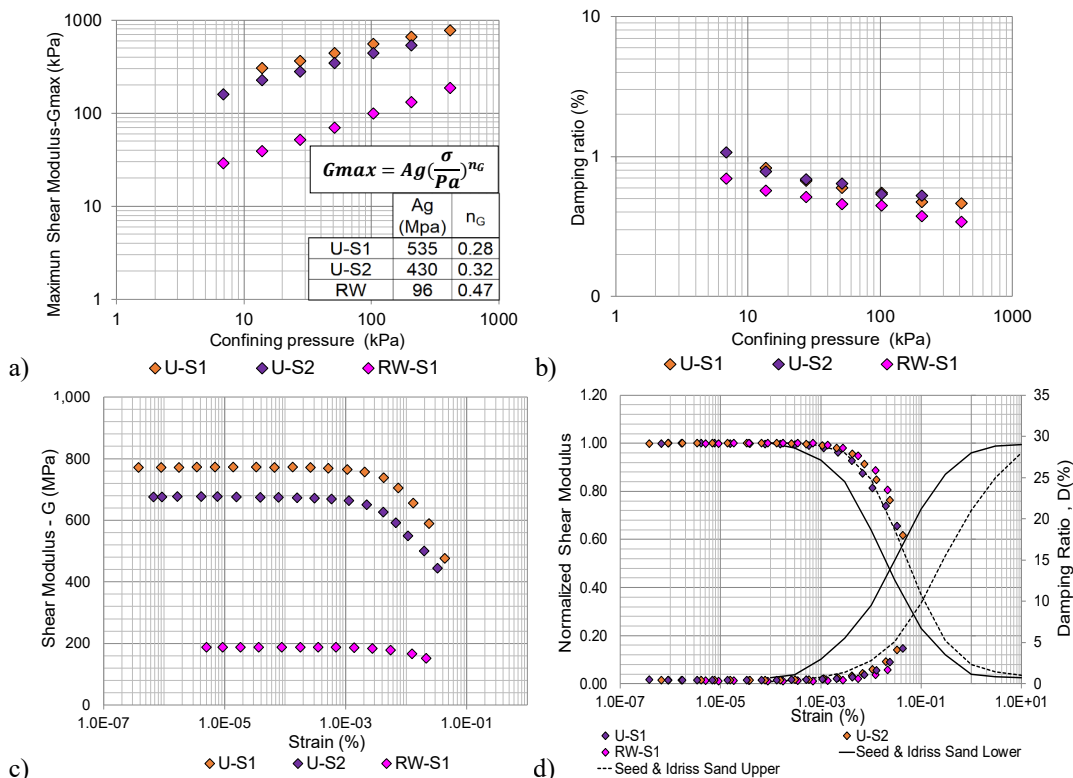


Figure 11. Resonant column results a) Maximum Shear Modules, b) Damping ratio, c) Shear modules vs. Strain and d) Normalized shear modules and damping ratio curves.

6.2 Liquefaction Resistance

Cyclic Direct Simple Shear (CDSS) tests were performed to obtain the liquefaction resistance curve of the material. For the sake of simulating potential collapse prior cyclic loading, due to the dissolution of the salts when the material is saturated, the specimens were reconstituted washed (RW) at the same dry density of the undisturbed Sample 1. The procedure consisted of consolidating the specimens to a desired vertical stress; with or without an initial static shear stress. Once the consolidation was complete; the vertical loading plate was locked in place (constant height testing) and the bottom plate was sheared under a harmonic sinusoidal loading at a frequency of 0.1Hz, with amplitude characterized by a defined Cyclic Stress Ratio (CSR).

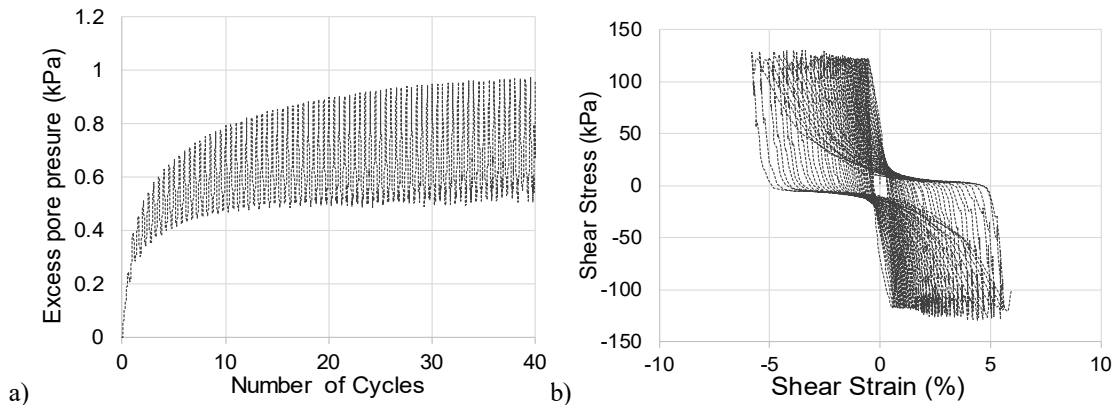


Figure 12. Results of CDSS for CSR = 0.30 at 400kPa and alpha=0.0 a) Excess pore pressures vs number of Cycles, b) Normalized Vertical stress vs shear strain.

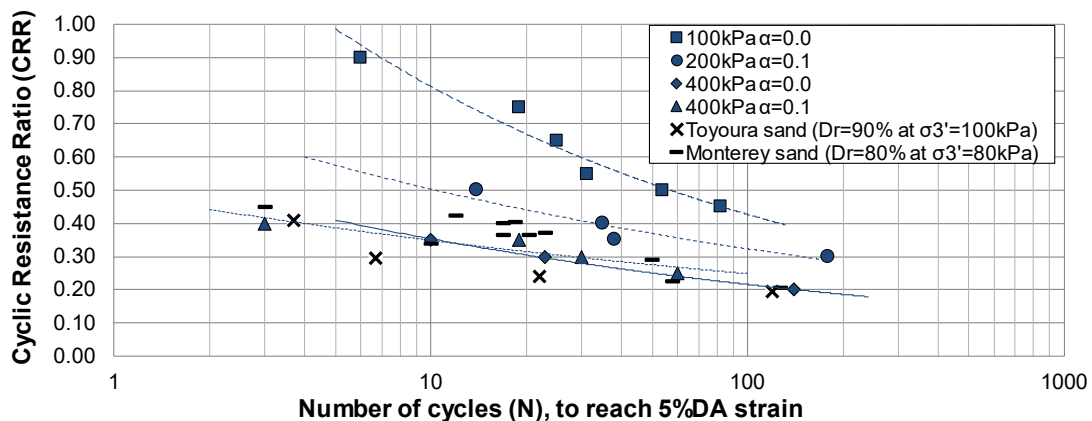


Figure 13. Liquefaction resistance curve for Collapsible Soils Type B ($D_r=80\%$) at different confining stresses and for other sands.

Due to the high relative density of the material, large strains were observed without reaching a total loss of effective stress. This is shown in Figure 12(b) (equivalent to normalized excess pore pressure generation $-R_u$ equal to 1.0). Therefore, a deformation criterion was chosen to identify the occurrence of liquefaction. Both, 5% and 10% double amplitude criteria were considered; however, there was not a significant difference between the results from the two criteria (this is consistent with findings by El Mohtar [2009]) and thus only the results based on the 5% double amplitude criterion is presented herein.

Figure 13 shows the number of cycles to the “failure” criterion plotted against the applied CSR for all of the CDSS tests performed in this study. A K_σ less than 1 was observed for this material due to the decrease in cyclic resistance with increasing confining stress. This behavior is common for the majority of natural sand deposits. Applying an initial shear stress during the consolidation phase resulted in a minor increase in the number of cycles to failure at confining stress of 400kPa. This is again consistent with previous studies for dense material ($K_\sigma > 1$) such as this (Idriss and Boulanger, 2008).

Cyclic resistance curves from other well-known sands are plotted to compare their response with Collapsible Soils Type B. The curves were chosen for samples with similar relative densities and confining stresses. These curves were for natural sands such as Toyoura sand with $D_r=90\%$ at $\sigma'_3=100\text{kPa}$ (Yamamoto et al, 2009) and Monterey sand with $D_r=80\%$ at $\sigma'_3=80\text{kPa}$ (Kammerer et al, 2004). The conclusion is that these natural sands, though having high relative densities, present much less cyclic resistance in comparison to Collapsible Soils Type B.

7 DISCUSSION AND CONCLUSION

- Based on laboratory tests, the typical behavior of Collapsible Soil Type A under shear loading is contractive (void ratio equal to 1.2); while Collapsible Soil Type B is generally dilatant (void ratio less than 0.70). This is also supported by in-situ field tests such as SPT.
- The impact of cementation on strength can be measured using CU and CD triaxial tests by performing tests on undisturbed specimens with and without water flushing. The impact of cementation can also be corroborated by comparing residual and peak failure envelopes for undisturbed specimens with crushed and washed specimens.
- Resonant column tests can be used to unravel the effects of cementation on the material stiffness. Dry undisturbed specimens presented a higher shear modulus than washed specimens. Also, the shear modulus for cemented sands is not affected by confining pressure as much as the shear modulus is for clean sands (lower n_G value).
- Collapsible Soils Type B present a much higher cyclic resistance (CRR) than Monterey and Toyoura sands with the same relative density and confining stress. It is suggested that this is a cementation effect.
- There was little difference between using a 5% or 10% double amplitude criteria for initial liquefaction of the samples subjected to CDSS loading.
- The liquefaction resistance of Collapsible Soils Type B are similar to that of typical sand (after removing cementation). Increasing the confining stresses trigger a decrease in cyclic resistance ($K\sigma < 1$), and an initial static shear causes a modest increase in the cyclic resistance ($K\alpha$).

REFERENCES

- ASTM Standard D.5333. 1996. Standard test method for measurement of collapse potential of soils. ASTM International, West Conshohocken, PA, 1996, www.astm.org.
- El Mohtar, C. 2009. Evaluation of the 5% Double Amplitude Strain Criterion. *International Conference on Soil Mechanics and Foundation Engineering, ISSMGE, October 2009*. Alexandria, Egypt
- Fear, C.E. and Robertson, P.K. 1995. Estimating the undrained strength of sand: a theoretical framework. *Canadian Geotechnical Journal*, 32, pp. 859-870.
- Idriss, I.M. & Boulanger, R.W. 2008. Soil Liquefaction during Earthquake. *EERI publication, Monograph MNO-12, Earthquake Engineering Research Institute*. Oakland, California, USA.
- Jefferies, M.G. & Been, K. 2015. Soil Liquefaction: A critical state approach, *Taylor and Francis*, Abingdon, ISBN 0-419-16170-8.
- Seed H.B. & Idriss I.M. 1970. Soil moduli and damping factors for dynamic response analyses. *Report No. EERC 70-10, Earthquake Engineering Research Center*, University of California, Berkeley, pp40.
- Yamamoto, Y., Hyodo, M. & Orense, R. 2009. Liquefaction resistance of sandy soils under partially drained condition, *Journal of Geotechnical and Geoenvironmental Engineering*, ASCE, Vol. 135, No. 8, 1032-1043.
- WU, J., Kammerer, A. M., Riemer, M. F., Seed, R. B. & Pestana, J. M. 2004. Laboratory study of liquefaction triggering criteria. *13th World Conference on Earthquake Engineering, Paper (No. 2580)*. Vancouver, BC, Canada.